Spectrochimica Acta Part A: Molecular and Biomolecular Spectroscopy 212 (2019) 232–239

Contents lists available at ScienceDirect

Spectrochimica Acta Part A: Molecular and Biomolecular Spectroscopy

journal homepage: www.elsevier.com/locate/saa

Poly(azomethine-urethane) and zeolite-based composite: Fluorescent biosensor for DNA detection

Umran Duru Kamaci [a], Musa Kamaci [b,*], Aysegul Peksel [a]

[a] Faculty of Arts and Sciences, Department of Chemistry, Yıldız Technical University, Esenler, 34220 Istanbul, Turkey
[b] Piri Reis University, Tuzla, 34940 Istanbul, Turkey

ARTICLE INFO

Article history:
Received 10 August 2018
Received in revised form 14 December 2018
Accepted 5 January 2019
Available online 6 January 2019

Keywords:
Zeolite
DNA
Fluorescent sensor
Biosensor

ABSTRACT

In the present paper, a highly selective and sensitive fluorescent biosensor based on poly(azomethine-urethane) and zeolite for the determination of DNA molecules was developed. Zeolite was chosen to enhance with anionic or cationic functional groups in polymer matrix and interaction between polymer and DNA. Several parameters such as polymer concentration, pH and incubation time effect on the sensitivity of the fluorescent biosensor were optimized. Linear range was determined between 2.50 and 25.00 nmol/L DNA concentration and limit of detection (LOD) of the biosensor was calculated as 0.095 nmol/L under the optimal conditions. Interference study was also performed in the presence of different amino acids, cations and organic compounds. The results clearly indicated that the tested cations and compounds were not induced a significant fluorescence change and the proposed zeolite-based biosensor was shown a good selectivity for DNA.

1. Introduction

The development of polymeric biosensor for the determination of deoxyribonucleic acid (DNA) molecules has attracted much attention in supramolecular chemistry within recent years due to vital function of DNA in transmitting, storing genetic information and protein biosynthesis [1–3]. DNA has excellent stability at atmospheric conditions and it has been founded many application areas due to these superior and vital properties [4]. Design of novel sensor for the determination of DNA molecules and DNA-drug interactions are still a need due to understand the effective reaction mechanism of drugs in human body. Also, reliable, sensitive, selective, rapid, economical, and practical detection of DNA molecules in any environment have been great importance.

Zeolites are porous crystalline aluminosilicate compounds and they are an important class of inorganic materials [5,6]. Zeolites have been used in a wide range application areas of industrial processes such as separation, adsorption, catalysis and ion-exchange [7,8]. Also, they have been found applications different types of sensors such as gas [9,10], humidity [11], formaldehyde [12], picric acid [13], glucose [14], urea [5] and H_2O_2 [15]. However, poly(azomethine-urethane) and zeolite-based composite for detection of DNA molecules as fluorescent biosensor was never mentioned in the literature.

In recent years, a variety of instrumental measurement methods such as acoustic [16], piezoelectric [17], colorimetric [18], fluorescence [19], optical [20] electrochemical [21], amperometric [22], voltammetric [23] and potentiometric [24] were used for determination of DNA molecules in different solutions or media. Among to these methods, fluorescence spectrophotometer is one of the most sensitive and selective method for the determination of biological molecules [2] and this method has some specific advantages such as detection speed, low cost, operation simplicity and in vivo and in vitro imaging possibility [25–27].

In this paper, a new fluorescent zeolite-based composite was prepared to detection of DNA molecules. In accordance with this purpose, a new fluorescent composite containing poly(azomethine-urethane) (PAMU) and zeolite was firstly prepared. Then, DNA molecules detection property of this composite as fluorescent biosensor was evaluated. Zeolite was used to enhance anionic or cationic functional groups in polymer matrix and interaction between polymer and DNA. Surface morphology of PAMU and zeolite-based composite was investigated by using SEM. Fluorescence measurement were also carried out to investigate the sensing property of zeolite-based composite.

2. Material and Methods

2.1. Materials

All compounds and solvents were supplied as commercially and they were used without purification. Calf thymus DNA (Type I), (3-aminopropyl)trimethoxysilane (APTMS), 2,4-dihydroxy benzaldehyde (2,4-DHBA), lysine diisocyanate ethyl ester (LDI), D-(+) glucose, L-tyrosine, L-aspartic acid, L-(+) ascorbic acid, dimethylformamide (DMF), ethanol (EtOH), tetrahydrofuran (THF), acetonitrile (MeCN), sodium

* Corresponding author at: Piri Reis University, Tuzla, 34940 Istanbul, Turkey
E-mail address: mkamaci@pirireis.edu.tr (M. Kamaci).

https://doi.org/10.1016/j.saa.2019.01.011
1386-1425/

phosphate monobasic ($NaH_2PO_4 \cdot 2H_2O$) and sodium phosphate dibasic ($Na_2HPO_4 \cdot 7H_2O$) were supplied from Sigma Aldrich. Powder sodium zeolite (Y-zeolite, $SiO_2/AlO_2 = 2.5$) was purchased from Zeolyst International. D-(−) Fructose was supplied from Riedel de Haen, L-cysteine, and L-tryptophan were supplied from Fluka.

2.2. Synthesis of (E)-4-(((3-(trimethoxysilyl)propyl)imino)methyl) benzene-1,3-diol

Prepolymer was prepared via condensation reaction of APTMS (0.414 g, 3 mmol) with 2,4-DHBA (0.538 g, 3 mmol) in 40 mL EtOH as shown in Fig. 1 and purified using recrystallization method from MeCN (1 × 25 mL) and distilled water (2 × 50 mL), and dried in a vacuum oven at 60 °C [28]. Yield: 86%.

2.3. Synthesis of Poly(azomethine-urethane)

Poly(azomethine-urethane) (PAMU) containing silane was prepared via step-polymerization reaction of the prepolymer (0.599 g, 2.0 mmol) with LDI (0.452 g, 2 mmol) as the following procedure: Prepolymer (0.599 g, 2.0 mmol) was dissolved in THF/DMF (3:2, v:v) mixture (60 mL) and placed in three-necked round bottom flask. LDI (0.452 g, 2.0 mmol) was dissolved in 20 mL THF and added to prepolymer solution. Then, reaction mixture was heated 90 °C and it maintained during 16 h under argon atmosphere in an oil bath. After 16 h, reaction mixture was cooled at room temperature and poly (azomethine-urethane) containing silane was precipitated, washed with water (3 × 50 mL) and MeOH (2 × 25 mL). Then, polymer was dried at 60 °C in vacuum oven overnight [29]. Yield: 89%; Mn: 18,400 Da, Mw: 21,500 Da, and PDI: 1.168.

2.4. Preparation of Poly(azomethine-urethane)-Zeolite Composite

Poly(azomethine-urethane)-zeolite composite (PAMU-zeolite) was prepared as follows: poly(azometine-urethane) containing silane (0.5 g) was dissolved in 60 mL THF/DMF mixture (3:2, v:v) and placed in two-necked round bottom flask. Zeolite (10.0 mg) was dissolved in 20 mL deionized water in ultrasonic bath sonicator during 30 min and added to polymer solution. Reaction was maintained during 72 h at room temperature. After 72 h, reaction mixture was precipitated, and washed with MeOH (2 × 25 mL) and deionized water (2 × 25 mL). Then, composite was dried at 60 °C in vacuum oven overnight [30]. Yield: 84%.

2.5. Measurements

The structural characterization of the prepolymer and its polymer was performed using a Perkin Elmer FT-IR Spectrum one with equipped the universal ATR sampling accessory in the range from 500 to 4000 cm^{-1}. A Bruker AC FT-NMR spectrometer (^1H NMR, 400.0 MHz; ^{13}C NMR, 100.6 MHz) were also used to characterize of these compounds in deuterated DMSO-d_6 at 25 °C in the presence of tetramethylsilane (TMS) as internal standard. The number average molecular weight (M_w) and PDI values were determined using a Shimadzu VP-10A gel permeation chromatography (GPC). A refractive index detector (RID) was used to analyze the polymer at 55 °C.

All of the fluorescence measurements were performed using a Perkin-Elmer LS 55 fluorescence spectrometer. Excitation wavelength and slit width were set at 480 and 5 nm in these measurements, respectively. UV–Vis spectra were recorded using a Schimadzu UV-1800 UV–Vis spectrophotometer.

SEM images of poly(azomethine-urethane) and poly(azomethine-urethane)-zeolite composite were investigated using a Zeiss EVO LS 10. For SEM measurements, the surface of PAMU and PAMU-zeolite composite was coated with a thin layer gold using a sputter coater prior to microscopy.

2.6. Preparation of DNA Stock Solution

DNA stock solution was prepared in 0.1 M phosphate buffer solution (PBS) according to the following procedure: 3 mg DNA was weighed and dissolved in 3 mL PBS. Then, absorption value of this solution was measured using a UV–vis spectroscopy at 260 nm and the concentration of the solution was calculated from the calculated molar extinction

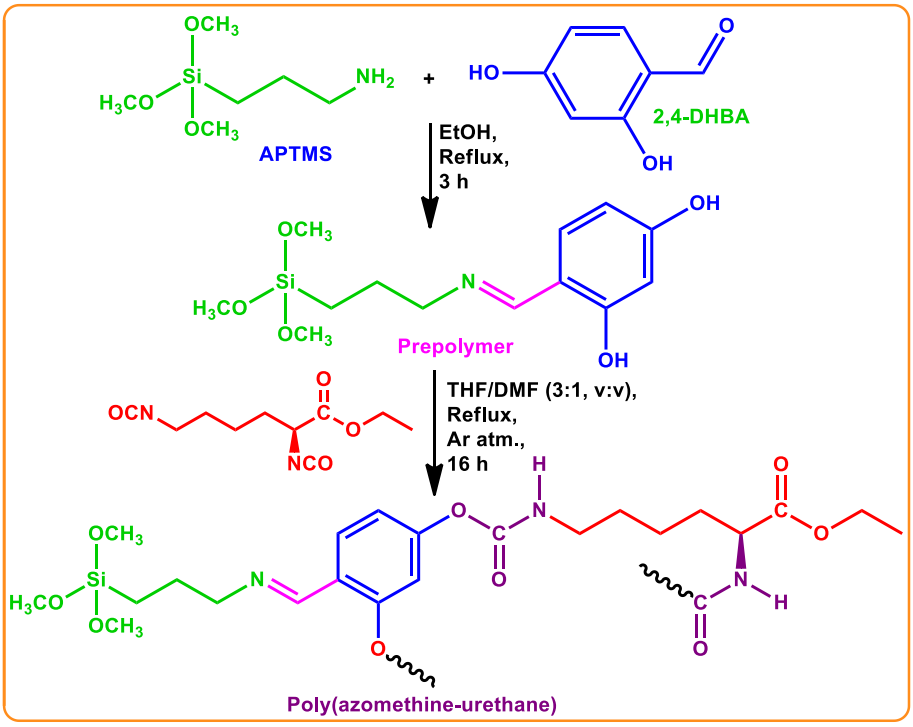

Fig. 1. Synthesis route of prepolymer and poly(azomethine-urethane).

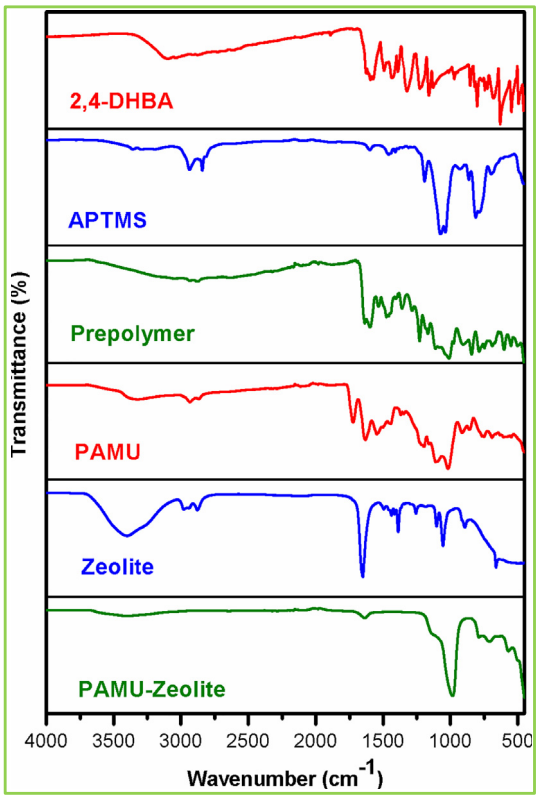

Fig. 2. FT-IR spectra of the starting materials, prepolymer, PAMU, zeolite and composite.

coefficient (ε) at the mentioned wavelength. Also, the stock solutions of DNA in the range from 0 to 60 nmol/L were prepared by dilution of this prepared solution in PBS.

3. Results and Discussion

3.1. Chemical Structures of Composite

FT-IR spectra of the starting materials, prepolymer, poly(azomethine-urethane) and composite were comparatively shown in Fig. 2 and results also given in Table 1. As can be seen in FT-IR data of 2,4-DHBA, characteristic hydroxyl (–OH) and aldehyde (–CHO) stretch vibrations were observed at 3098 and 1708 cm^{-1}, respectively. Characteristic amine ($–NH_2$) stretch vibration of APTMS was also recorded at 3305 cm^{-1}. These amine ($–NH_2$) stretch vibration of APTMS and aldehyde (–CHO) stretch vibration of 2,4-DHBA were disappeared due to imine (–N═CH) formation and this stretch vibration was seen at 1599 cm^{-1} in the structure of the prepolymer. In addition, hydroxyl (–OH) stretch vibration of the prepolymer was observed at 3169 cm^{-1}. According to FT-IR spectra of LDI, characteristic isocyanate –C═O and –C═N stretch vibrations were recorded at 2240 and 1461 cm^{-1}, respectively. In FT-IR spectrum of poly(azomethine-urethane), isocyanate stretch vibrations (–C═O and –C═N) of LDI and hydroxyl stretch vibration (–OH) of the prepolymer were disappeared due to urethane (-NH-COO) formation. Urethane –NH and –C═O stretch vibrations were observed at 3358 and 1731 cm^{-1}, respectively. Moreover, imine (–N═CH) stretch vibration of PAMU was observed at 1640 cm^{-1}. These results clearly showed that imine (N═CH) stretch vibration of PAMU was shifted to higher frequency due to formation of urethane bond. In the FT-IR spectrum of zeolite, silanol (–Si-OH), hydroxyl (–OH) and Al—O or Si—O stretch vibrations were seen at 3407, 1654 and 1055 cm^{-1}, respectively [31]. According to FT-IR spectrum of poly(azomethine-urethane)-zeolite composite these stretch vibrations were observed at 3041, 1645 and 986 cm^{-1}, respectively. Silanol (–Si-OH) and hydroxyl (–OH) stretch vibrations were observed as wide and strong peaks in the structure of composite and these vibrations were overlapped to urethane –NH and –C═O vibrations. Because of these properties urethane –C═O and –NH stretch vibrations were not observed in the structure of PAMU-zeolite composite. In addition, imine stretch vibration of composite was observed at 1638 cm^{-1}.

^1H NMR and ^{13}C NMR data of the prepolymer and poly(azomethine-urethane) were summarized in Table 2. Hydroxyl (–OH) proton of the prepolymer was observed at 10.45 ppm and imine (–N═CH) proton seen at 9.12 ppm. Methoxy proton ($–OCH_3$) in the structure of prepolymer was also recorded at 3.66 ppm. Moreover, aromatic –CH (Ar-CH) and aliphatic –CH (Al-CH) protons were observed in the range from 7.21 to 7.93 ppm and 1.10 to 3.98 ppm, respectively. According to ^1H NMR data of poly(azomethine-urethane), urethane (–NH), imine (–N═CH) and methoxy ($–OCH_3$) protons were recorded at 9.64, 9.47 and 3.69 ppm, respectively. Ar-CH and Al-CH protons in the

Table 2
^1H NMR and ^{13}C NMR data of prepolymer and poly(azomethine-urethane).

Compounds	δ (ppm)
Prepolymer	^1H NMR (400 MHz, DMSO-d_6): 10.45 (s, hydroxyl, –OH), 9.12 (s, imine, –N═CH), 7.93 (d, Ar-CH), 7.64 (d, Ar-CH), 7.21 (d, Ar-CH), 3.98 (d, Al-CH), 3.66 (t, methoxy, $–OCH_3$), 1.97 (d, Al-CH) and 1.10 (d, Al-CH). ^{13}C NMR (100.6 MHz, DMSO-d_6): 164.8 (hydroxyl-C-OH), 158.7 (imine, –N═CH), 155.8 (*ipso*, Ar-CH), 138.7 (Ar-CH), 119.2 (Ar-CH), 108.9 (Ar-CH), 103.7 (Ar-CH), 66.8 (Al-CH), 50.2 (methoxy, $–OCH_3$), 20.2 (Al-CH) and 14.4 (Al-CH).
Poly (azomethine-urethane)	^1H NMR (400 MHz, DMSO-d_6): 9.64 (s, urethane, –NH), 9.47 (s, imine, –N═CH), 8.08 (d, Ar-CH), 7.79 (d, Ar-CH), 7.27 (d, Ar-CH), 4.72 (s, Al-CH), 4.33 (d, Al-CH), 4.02 (d, Al-CH), 3.69 (t, methoxy, $–OCH_3$), 3.27 (d, Al-CH), 2.03 (d, Al-CH), 1.90 (d, Al-CH), 1.38 (d, Al-CH), 1.29 (s, $–CH_3$), 1.21 (d, Al-CH) and 1.14 (d, Al-CH). ^{13}C NMR (100.6 MHz, DMSO-d_6): 170.8 (–C═O, diisocyanate), 161.7 (urethane, –C═O), 159.3 (imine, –N═CH), 151.8 (*ipso*, Ar-CH), 148.7 (*ipso*, Ar-CH), 134.5 (Ar-CH), 122.5 (Ar-CH), 114.0 (Ar-CH), 110.4 (Ar-CH), 67.1 (Al-CH), 61.3 (Al-CH), 57.1 (Al-CH), 56.8 (Al-CH), 50.4 (methoxy, $–OCH_3$), 40.3 (Al-CH), 31.1 (Al-CH), 29.6 (Al-CH), 22.8 (Al-CH), 15.9 (Al-CH) and 13.8 (Al-CH).

Table 1
FT-IR data of the starting materials, prepolymer, poly(azomethine-urethane) and composite.

Compounds	Urethane –NH	Urethane –C═O	Imine –N═CH	Hydroxyl –OH	Silanol	–OH	Al—O or Si—O	Aldehyde –CHO	Amine $–NH_2$
2,4-DHBA	–	–	–	3098	–	–	–	1708	
APTMS	–	–	–	–	–	–	–	–	3305
Prepolymer	–	–	1599	3169	–	–	–	–	–
PAMU	3358	1731	1640	–	–	–	–	–	–
Zeolite	–	–	–	–	3407	1654	1055	–	–
Composite	–	–	1638	–	3401	1645	986	–	–

structure of the polymer were seen in the range from 7.27 to 8.08 ppm and 1.14 to 4.72 ppm, respectively. These results indicated that imine (–N═CH) proton of polymer was shifted to low field after urethane bond formation.

As can be seen in ^{13}C NMR data of the prepolymer, hydroxyl (–C-OH), imine (–N═CH) and methoxy (–OCH_3) carbons were observed at 164.8, 158.7 and 50.2 ppm, respectively. Urethane –C═O, imine (–N═CH) and methoxy (–OCH_3) carbons of poly(azomethine-urethane) were recorded at 170.8, 161.7 and 50.4 ppm, respectively. Moreover, some additional carbon peaks such as aromatic and aliphatic carbons of prepolymer and polymers were observed in the range from 103.7 to 155.8 and 13.8 to 67.1 ppm, respectively. These FT-IR and NMR results were confirmed the structures of the prepolymer and poly (azomethine-urethane) as shown in Fig. 1.

3.2. Surface Morphology

Surface morphology of poly(azomethine-urethane) and polymer-zeolite composite was examined by scanning electron microscope (SEM) and SEM images of the compounds were comparatively given in Fig. 3 at different magnitude. As can be seen in SEM images of poly (azomethine-urethane) (Fig. 3a, c and e), PAMU was composed of a smooth surface. SEM images of polymer-zeolite composite (Fig. 3b, d and f) clearly demonstrated that zeolite was properly mixed with polymer matrix and it uniformly dispersed in poly(azomethine-urethane) (PU) matrix with a smooth surface.

3.3. Fluorescence Properties

To examine fluorescence properties of DNA, the interaction of DNA with poly(azomethine-urethane) and composite were given in Fig. 4. DNA, polymer and composite concentrations were adjusted as 25 nmol/L, 20 μg/mL and 20 μg/mL, respectively. Emission intensities of DNA, polymer-DNA and composite-DNA were determined as 46, 160 and 244, respectively. These results clearly indicated that the emission intensity, the interaction of composite-DNA was the higher emission intensity than polymer-DNA interaction due to cationic and anionic functional groups of zeolite in the structure.

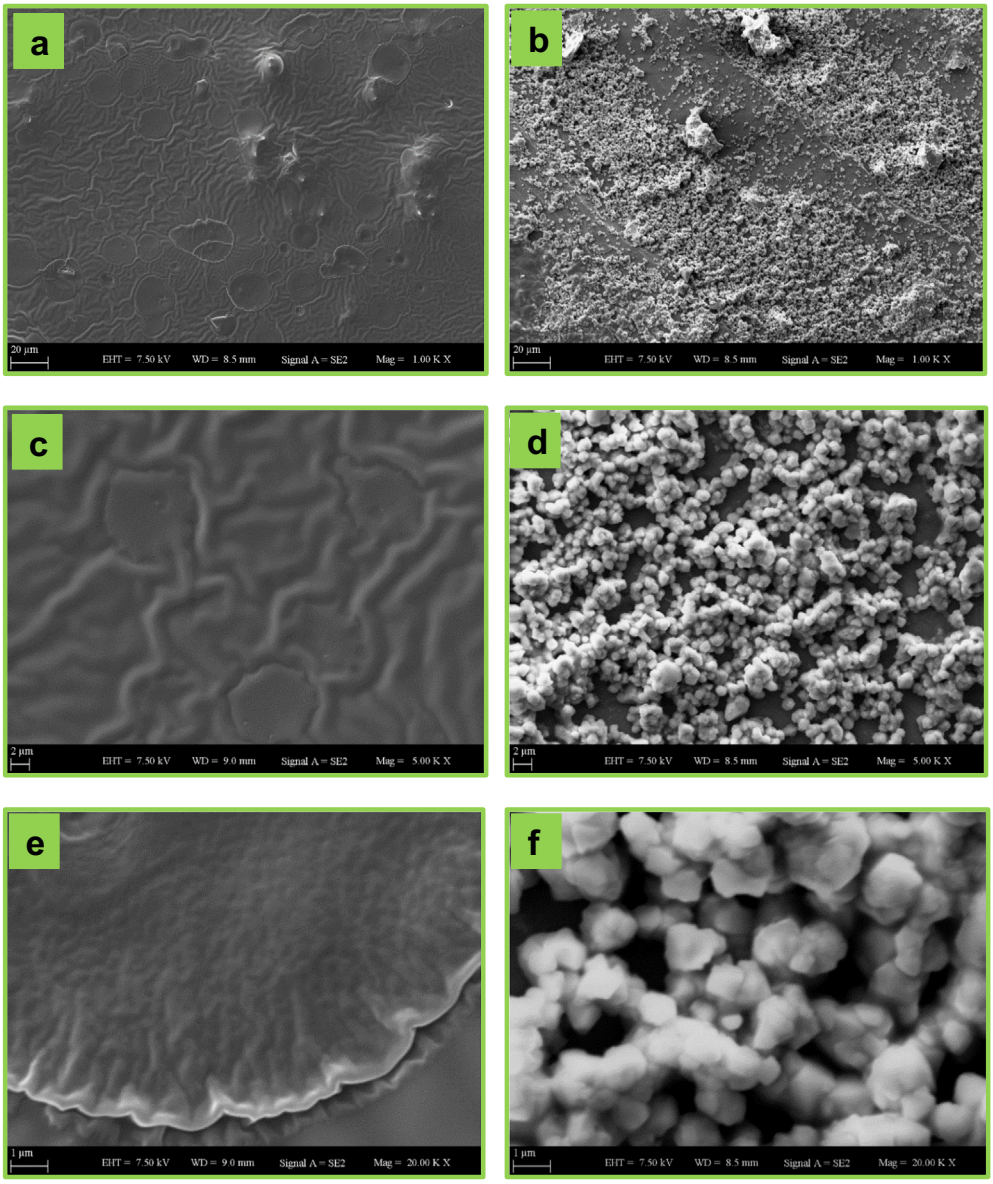

Fig. 3. SEM images of PAMU (a, c, e) and zeolite-based composite (b, d, f) at different magnitude (1, 5 and 20 k×).

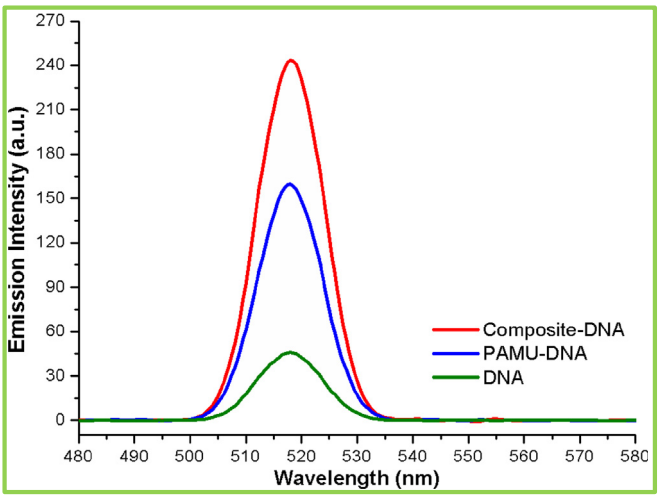

Fig. 4. Fluorescence spectra of DNA, polymer-DNA and composite-DNA.

3.4. Optimization Studies

In order to evaluate optimal experimental condition, optimization studies as composite concentration, pH and incubation time were carried out. These optimization studies were performed in 0.1 M PBS. This buffer solution was prepared using $NaH_2PO_4 \cdot 2H_2O$ and $Na_2HPO_4 \cdot 7H_2O$ salts at different pH and it was also used to prepare DNA and PAMU-zeolite stock solutions. In addition, slit was adjusted as 10 nm in these measurements.

Fig. 5a shows PAMU-zeolite composite concentration effect on emission intensity in the presence of 5 nmol/L DNA concentration. Composite solutions (5–60 μg/mL) were prepared in DMF/PBS (10:90; v:v). The results clearly showed that emission intensity difference ($\Delta F = F - F_o$, where F and F_o are emission intensities of composite biosensor in the presence and absence of DNA) of PAMU-zeolite composite was increased with the increase of composite concentration in the range from 10 μg/mL to 40 μg/mL while this difference decreased after 50 μg/mL composite concentration. As can be seen in Fig. 4a, emission intensity difference (ΔF) of PAMU-zeolite composite concentration for 10, 20, 30, 40, 50 and 60 μg/mL was determine as 160, 165, 205, 230,168 and 166, respectively. According to these results 40 μg/mL composite concentration has higher emission intensity and this concentration (40 μg/mL) was selected as an optimum composite concentration the further measurements.

Fig. 5b shows pH effect on emission intensity in the presence of 5 nmol/L DNA solution and 40 μg/mL PAMU-zeolite solution. In these measurements were performed between 6.8 and 7.8 pH range in 0.1 M PBS. Emission intensity difference ($F - F_o$) of the fluorescent biosensor was decreased in the range from 6.8 to 7.2 and 7.6 to 7.8 pH range. The reason of fluctuation in emission intensities at different pH media was due to partial denaturation of DNA in these pH media [32]. In addition, the highest emission intensity difference (ΔF) was obtained at pH 7.4 and this pH value was selected as an optimum pH the further measurements. The obtained results were in accordance with literature [33].

Incubation time effect on emission intensity of the fluorescent sensor was given in Fig. 5c in the presence of 5 nmol/L DNA solution and 40 μg/mL PAMU-zeolite solution. Emission intensity difference (ΔF) increased with the increase of incubation time until 15 min. After 15 min incubation time, emission intensity difference was decreased between 20 and 30 min. Maximum emission intensity difference (ΔF) was determined as 226 for 15 min incubation time and this time was selected as an optimum incubation time the further measurements.

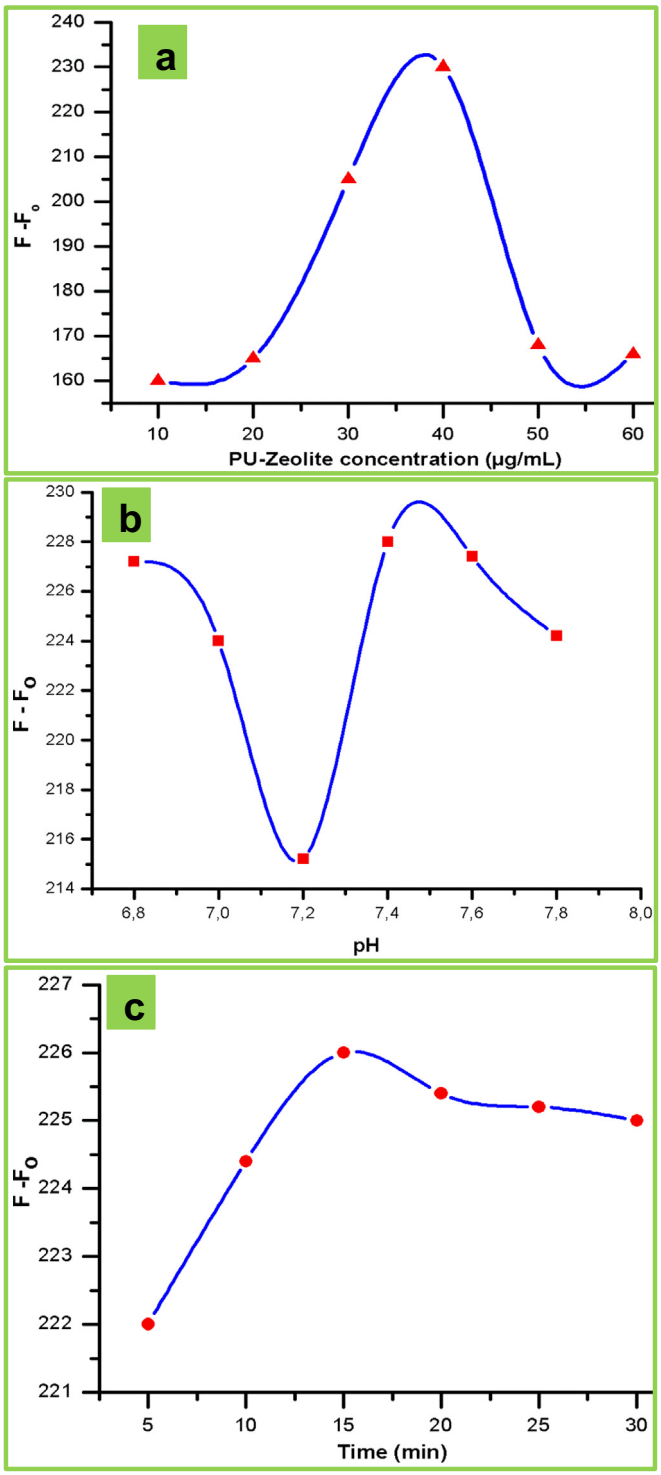

Fig. 5. Composite (a), pH (b) and incubation time (c) effect on fluorescence intensity difference.

3.5. Fluorescence Properties of PAMU and Composite

Fluorescence measurements of poly(azomethine-urethane) and zeolite-based composite were carried out to investigate fluorescence behavior of PAMU and zeolite-based composite. Fluorescence measurements indicated that PAMU has emission intensity at 518 nm about 56 (a.u.) and emission intensity of zeolite-based composite was a bit increased around 83 (a.u.) when compared the emission intensity of PAMU at this wavelength.

3.6. DNA Concentration Effect on Poly(azomethine-urethane)-Zeolite Composite

To determine the interaction of poly(azomethine-urethane)-zeolite composite with DNA, fluorescence measurements were performed under above the optimal conditions due to determine response range and detection limit in the presence of the different DNA amounts (0–60 nmol/L) (Fig. 6a). As shown in Fig. 6a, the fluorescence intensity difference (ΔF) was directly proportional to increasing amount of DNA molecules (added into the composite solution) in the range 2.5 to 25 nmol/L. Moreover, ΔF not linearly changed between 30 and 60 nmol/L DNA concentrations.

The relationship between the difference of fluorescence intensity (ΔF) and the concentration of DNA molecules was given in Fig. 6b as the calibration curve under the optimal conditions. The regression equation was determined as $\Delta F = 6.4108[DNA] + 82.618$ and regression coefficient was found as $R^2 = 0.9925$. As can be seen in Fig. 6b, the fluorescence response of zeolite-based composite was gradually increased in the different concentration of DNA and linear range of the fluorescent biosensor to DNA was determined in the 2.5 to 25 nmol/L. These results clearly showed that there was a good linear relationship between fluorescence intensity difference and DNA concentration at the mentioned range.

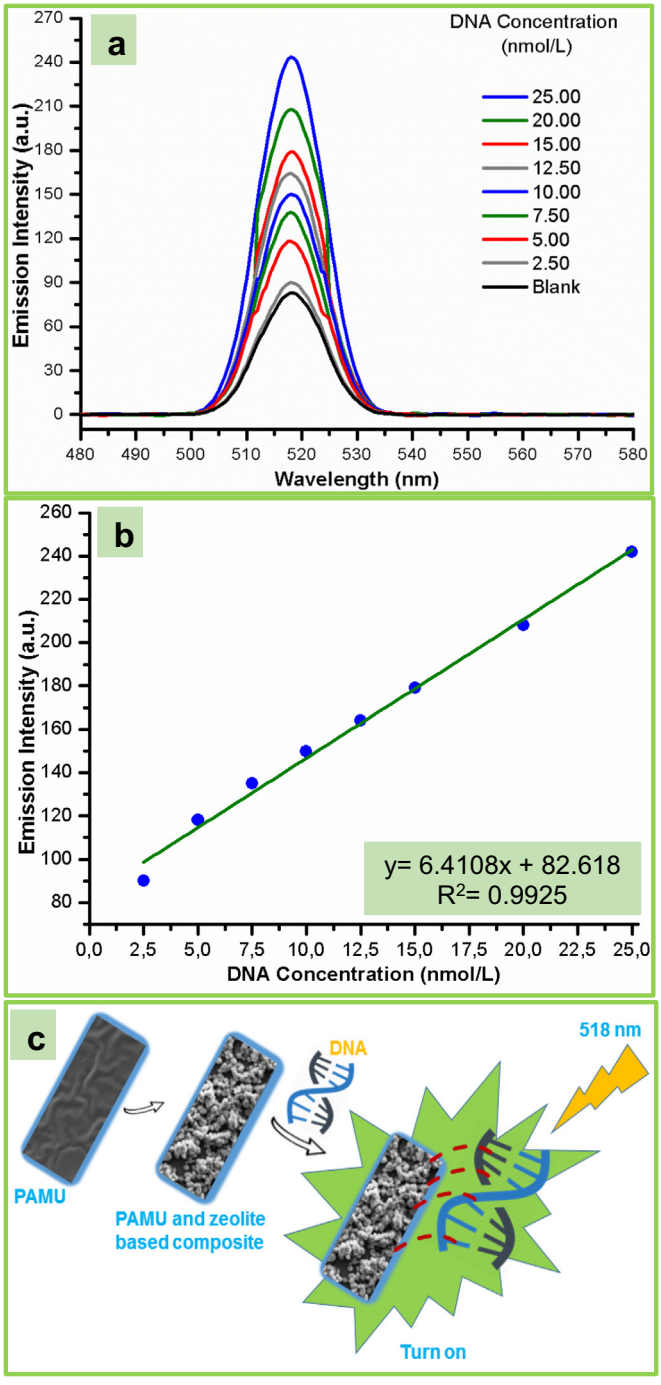

Fig. 6. (a) Fluorescence spectra of zeolite-based composite in the presence of different DNA concentrations, (b) linear relationship between DNA concentrations and fluorescence intensity difference above the optimal conditions and (c) schematic representation for the proposed biosensor.

3.7. Limit of Detection

Limit of detection (LOD) of the fluorescence response of composite biosensor was calculated by using fluorescence titration method as the following equation [26]:

$$LOD = \frac{3\sigma_{bi}}{m}. \quad (1)$$

where σ_{bi} and m are standard deviation of blank measurements and slope value the obtained from Fig. 5. To determine standard deviation (σ_{bi}), the emission intensity of PAMU-zeolite composite was measured 10 times in the absence of DNA in DMF/PBS (10:90; v:v). The emission intensities of composite were measured as 82.852, 82.308, 82.422, 82.398, 82.756, 82.928, 82.588, 82.705, 82.825 and 82.498. Standard deviation (σ_{bi}) value of composite fluorescent biosensor was also calculated as 0.204. Moreover, LOD value of the fluorescent biosensor was calculated as 0.095 nmol/L (95.46 pmol/L).

3.8. UV–Vis Spectra and Binding Interaction Type

To investigate binding interaction type and the structural transitions of DNA, UV–Vis absorption measurements were performed and UV–Vis absorption spectra of DNA, composite and DNA-composite mixture comparatively given in Fig. 7. These absorption measurements were performed in the presence of 40 μg/mL zeolite-based composite and 10 nmol/L DNA. The absorption peak of DNA and DNA-composite mixture was appeared at 260 nm and 266 nm, respectively, while zeolite-based composite absorption peak observed at 270 nm and. 6 nm red shift was observed at PAMU-zeolite composite absorption peak in the presence of DNA solution. Ensafi et al. reported that large change in the absorption peak and red shift in the wavelength lower than 15 nm

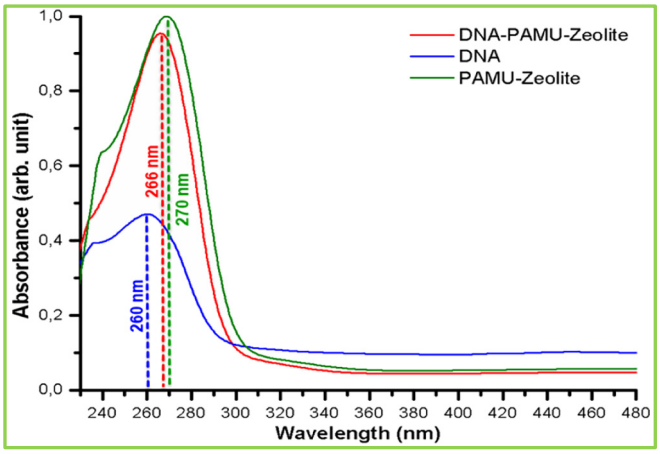

Fig. 7. UV–Vis spectra of DNA, zeolite-based composite and DNA-composite mixture above the optimal conditions.

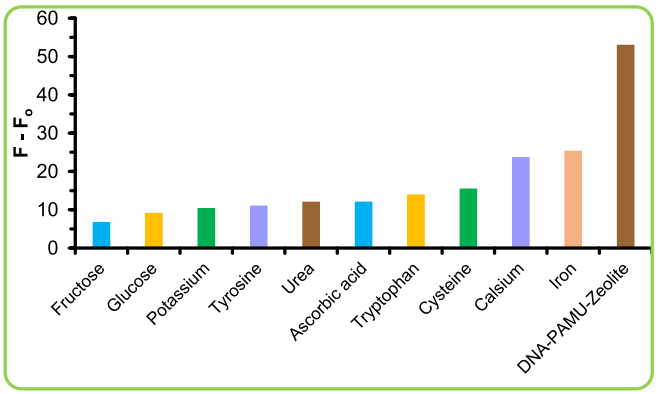

Fig. 8. Fluorescence response of the proposed biosensor to different amino acids, cations and organic compounds above the optimal conditions.

were defined as intercalation binding [33]. These explanations clearly indicated that the binding interaction type between DNA and zeolite-based composite was intercalation.

3.9. Selectivity

Interference effect of some amino acids (cysteine, tyrosine and tryptophan), cations (Ca^{2+}, K^{+} and Fe^{3+}), and organic compounds (ascorbic acid, fructose, glucose and urea) that might exist in real sample on the proposed fluorescent sensor was investigated (Fig. 8) in the presence of 40 μg/mL zeolite-based composite and 10 nmol/L DNA. Urea concentration was adjusted as 50 μg/mL, ascorbic acid, glucose and fructose concentrations were adjusted as 100 μg/mL, Ca^{2+}, Fe^{3+}, cysteine, tryptophan and tyrosine was adjusted as 200 μg/mL, and K^{+} ion concentration was adjusted as 300 μg/mL in these measurements using 0.1 M PBS. The tested amino acids such as cysteine, tyrosine and tryptophan was not exhibited a considerable effect on zeolite-based composite biosensor. The tested ions such as Ca^{2+}, K^{+} and Fe^{3+} were not caused a significant change in interference change on the proposed fluorescence biosensor system. Also, the tested organic compounds such as ascorbic acid, fructose, glucose and urea were not highly affected on interference value of the biosensor. As can be seen interference results, the proposed biosensor only exhibited recover response to DNA molecules and the tested amino acids, cations or organic compounds were not induced a significant fluorescence change. These interference results confirmed that zeolite-based biosensor was shown a good selectivity toward DNA molecules.

Moreover, limit of detection (LOD) and linear range results of zeolite-based composite biosensor were compared with other papers for the detection of DNA molecules. LOD and linear range results were compared only two articles (Table 3) due to the limitations of zeolite or zeolite composite-based papers for the detection of DNA molecules [1,34]. As shown in Table 3, zeolite-based composite biosensor has a comparable, good limit of detection and linear range.

3.10. Analytical Application

To investigate the practicability of the biosensor, five synthetic samples containing amino acid, cations or organic compound were tested (Table 4) by using standard addition method. According to Table 4, the recoveries were found in the range from 98.2 to 101.3% and relative standard deviation (RSD, n = 3) determined between 1.18 and 2.45%. The proposed zeolite-based composite sensor could be applied to detect DNA molecules in analytical applications with practical, reliable and satisfied results.

4. Conclusion

In this paper, a novel zeolite and poly(azomethine-urethane) based composite fluorescent sensing system to determination of DNA was developed with easy, fast, sensitive, selective and reliable. To determine DNA sensing performance of the zeolite-based composite, the optimal conditions such as the composite concentration, pH and incubation time were investigated. LOD value of the biosensor was calculated using fluorescence titration methods and it found as 95.46 pmol/L and linear range determined as 2.5–25 nmol/L. Also, binding interaction type between DNA and composite was found to be intercalation type. Analytical applications were also tested in the presence of different synthetic samples and the recoveries were found in the range from 98.2 to 101.3% and RSD determined between 1.18 and 2.45%.

References

[1] H. Song, S. Huo, J. Dong, J. Xu, An electrochemical sensor based on gold nanoparticles incorporated in mesoporous MFI zeolite for determination of purine bases in DNA, Electroanalysis 29 (2017) 1–9.
[2] R. Huang, N. Hea, Z. Li, Recent progresses in DNA nanostructure-based biosensors for detection of tumor markers, Biosens. Bioelectron. 109 (2018) 27–34.
[3] W. Wei, C. Gao, Y. Xiong, Y. Zhang, S. Liu, Y. Pu, A fluorescence method for detection of DNA and DNA methylation based on graphene oxide and restriction endonuclease HpaII, Talanta 131 (2015) 342–347.
[4] F. Geng, X. Jiang, Y. Wang, C. Shao, K. Wang, P. Qu, M. Xu, DNA-based dual fluorescence signals on and ratiometric mercury sensing in fetal calf serum with simultaneous excitation, Sensors Actuators B Chem. 260 (2018) 793–799.
[5] D.E. Anderson, S. Balapangu, H.N.A. Fleischer, R.A. Viade, F.D. Krampa, P. Kanyong, G.A. Awandare, E.K. Tiburu, Investigating the influence of temperature on the

Table 3
Comparison of zeolite-based biosensors for the determination of DNA.

Materials	Method	Detection limit	Linear range	Reference
Ag/NaA zeolite	Voltammetric	4 pmol/L	0.002–0.008 nmol/L	[34]
Gold NP-zeolite	Electrochemical	0.25 μmol/L 0.29 μmol/L	0.5–500 μmol/L 0.8–500 μmol/L	[1]
PAMU-zeolite	Fluorescence	95.46 pmol/L	2.50–25.00 nmol/L	This study

Table 4
Analytical application of DNA determination in different samples.

Sample	Foreign substance (μg/mL)	DNA added (μg/mL)	DNA founded (μg/mL)	Recovery (%)	R.S.D.[a] (%)
1	K^{+} (300), glucose (100), cysteine (200)	6.0	5.98	99.7	1.18
2	Ca^{2+} (200), ascorbic acid (100), tryptophan (200)	6.0	5.89	98.2	1.51
3	K^{+} (300), urea (50), cysteine (200)	6.0	5.94	99.0	1.69
4	Ca^{2+} (200), urea (50), tryptophan (200)	6.0	6.03	100.5	2.45
5	K^{+} (300), fructose (100), tyrosine (200)	6.0	6.08	101.3	1.23

[a] Relative standard deviation.

kaolinite-base synthesis of zeolite and urease immobilization for the potential fabrication of electrochemical urea biosensors, Sensors 17 (2017) 1831.
[6] X. Zhang, J. Sun, J. Liu, H. Xu, B. Dong, X. Sun, T. Zhang, S. Xu, L. Xu, X. Bai, S. Zhang, S. Mintova, G. Lu, H. Song, Label-free electrochemical immunosensor based on conductive Ag contained EMT-style nano-zeolites and the application for α-fetoprotein detection, Sensors Actuators B Chem. 255 ((2018) 2919–2926.
[7] T.J. Barton, L.M. Bull, W.G. Klemperer, D.A. Loy, B. McEnaney, M. Misono, P.A. Monson, G. Pez, G.W. Scherer, J.C. Vartuli, O.M. Yaghi, Tailored porous materials, Chem. Mater. 11 (1999) 2633–2656.
[8] B. Chen, Z. Yang, Y. Zhu, Y. Xia, Zeolitic imidazolate framework materials: recent progress in synthesis and applications, J. Mater. Chem. A 2 (2014) 16811–16831.
[9] S. Galioglu, I. Karaduman, T. Çorlu, B. Akata, M.A. Yıldırım, A. Ateş, S. Acar, Zeolite a coated $Zn_{1-x}Cu_xO$ MOS sensors for NO gas detection, J. Mater. Sci. Mater. Electron. 29 (2018) 1356–1368.
[10] M. Denoual, D. Robbes, S. Inoue, Y. Mita, J. Grand, H. Awala, S. Mintova, Thermal resonant zeolite-based gas sensor, Sensors Actuators B Chem. 245 (2017) 179–182.
[11] Y. Zang, H.Y. Xiang, L. Sun, Q.H. Xie, M. Liu, Y. Chen, S.P. Ruan, A sensor based on LiCl/NaA zeolite composites for effective humidity sensing, J. Nanosci. Nanotechnol. 18 (2018) 1882–1886.
[12] A.T. Guntner, S. Abegg, K. Wegner, S.E. Pratsinis, Zeolite membranes for highly selective formaldehyde sensors, Sensors Actuators B Chem. 257 (2018) 916–923.
[13] B.L. Wang, Y. Mu, C.H. Zhang, J.Y. Li, Blue photoluminescent carbon nanodots prepared from zeolite as efficient sensors for picric acid detection, Sensors Actuators B Chem. 253 (2017) 911–917.
[14] J. Dong, T. Tian, L. Ren, Y. Zhang, J. Xu, X. Cheng, CuO nanoparticles incorporated in hierarchical MFI zeolite as highly active electrocatalyst for non-enzymatic glucose sensing, Colloids Surf. B 125 (2015) 206–212.
[15] H. Ramezani, S.N. Azizi, S.R. Hosseini, NaY zeolite as a platform for preparation of Ag nanoparticles arrays in order to construction of H_2O_2 sensor, Sensors Actuators B Chem. 248 (2017) 571–579.
[16] Y. Zhang, F. Yang, Z. Sun, Y. Li, G. Zhang, A surface acoustic wave biosensor synergizing DNA-mediated *in situ* silver nanoparticle growth for a highly specific and signal-amplified nucleic acid assay, Analyst 142 (2017) 3468–3476.
[17] S. Kim, S.J. Choi, A lipid-based method for the preparation of a piezoelectric DNA biosensor, Anal. Biochem. 458 (2014) 1–3.
[18] G. Tang, J. Gao, C. Wang, H. Tan, Luminescent lanthanide coordination polymer as a platform for DNA colorimetric detection, Sensors Actuators B Chem. 244 (2017) 571–576.
[19] A. Narmani, M. Kamali, B. Amini, H. Kooshki, A. Amini, L. Hasani, Highly sensitive and accurate detection of *Vibrio cholera* O1 OmpW gene by fluorescence DNA biosensor based on gold and magnetic nanoparticles, Process Biochem. 65 (2018) 46–54.
[20] R.P. Talemi, M.H. Mashhadizade, A novel optical DNA biosensor for detection of trace concentration of methylene blue using gold nano-particles and Guanine rich single strand DNA, Int. J. Nano Dimens. 8 (2017) 224–233.
[21] M. Arvand, M. Sanayeei, S. Hemmati, Label-free electrochemical DNA biosensor for guanine and adenine by ds-DNA/poly(L-cysteine)/Fe_3O_4 nanoparticles-graphene oxide nanocomposite modified electrode, Biosens. Bioelectron. 102 (2018) 70–79.
[22] Z. Ölcer, E. Esen, A. Ersoy, S. Budak, D.S. Kaya, M.Y. Gök, S. Barut, D. Üstek, Y. Uludag, Microfluidics and nanoparticles based amperometric biosensor for the detection of cyanobacteria (*Planktothrix agardhii* NIVA-CYA116) DNA, Biosens. Bioelectron. 70 (2015) 426–432.
[23] L.E. Ahangar, M.A. Mehrgardi, Nanoporous gold electrode as a platform for the construction of an electrochemical DNA hybridization biosensor, Biosens. Bioelectron. 38 (2012) 252–257.
[24] X.L. Zong, C.S. Wu, X.L. Wu, Y.F. Lu, P. Wang, Non-labeled DNA biosensor based on light addressable potentiometric sensor modified with TiO_2 thin film, J Zhejiang Univ Sci B 10 (2009) 860–866.
[25] S. Li, J. Li, J. Luo, Q. Zhang, L. Zhang, A fluorescence switch sensor for detection of virginiamycin based on graphene oxide-supported carbon quantum dots and molecularly imprinted polymer, RSC Adv. 7 (2017) 56359–56364.
[26] M. Kamaci, I. Kaya, A highly selective, sensitive and stable fluorescent chemosensor based on Schiff base and poly(azomethine-urethane) for Fe^{3+} ions, J. Ind. Eng. Chem. 46 (2017) 234–243.
[27] H. Xu, F. Geng, X. Jiang, C. Shao, Y. Wang, K. Wang, P. Qu, M. Xu, B.C. Ye, Design of metal-ion-triggered assembly of label-free split G-quadruplex/duplex DNA for turn-on detection of Hg^{2+} in fetal calf serum, Sensors Actuators B Chem. 255 (2018) 1024–1030.
[28] U. Duru Kamaci, M. Kamaci, A. Peksel, Thermally stable Schiff base and its metal complexes: molecular docking and protein binding studies, J. Fluoresc. 27 (2017) 805–817.
[29] M. Kamaci, I. Kaya, New low-band gap polyurethanes containing azomethine bonding: photophysical, electrochemical, thermal and morphological properties, J. Taiwan Inst. Chem. Eng. 59 (2016) 536–546.
[30] B.V.S. Kumar, M.B. Siddaramaiah, K.S. Shayan, C. Manjula, G.V.N. Ranganathaiah, B. Rao, K. Byrappa Basavalingu, Effect of zeolite particulate filler on the properties of polyurethane composites, J. Polym. Res. 17 (2010) 135–142.
[31] H. Jahangirian, M.H.S. Ismail, M.D.J. Haron, R.R. Moghaddam, K. Shameli, S. Hosseini, K. Kalantari, R. Khandanlou, E. Gharibshahi, S. Soltaninejad, Synthesis and characterization of zeolite/Fe_3O_4 nanocomposite by green quick precipitation method, Dig. J. Nanomater. Biostruct. 8 (2013) 1405–1413.
[32] M. Malavasic, N. Poklar, P. Macek, G. Vesnaver, Fluorescence studies of the effect of pH, guanidine hydrochloride and urea on equinatoxin II conformation, Biochim. Biophys. Acta 1280 (1996) 65–72.
[33] A.A. Ensafi, P. Nasr-Esfahani, B. Rezaei, Quenching-recovery fluorescent biosensor for DNA detection based on mercaptopropionic acid-capped cadmium telluride quantum dots aggregation, Sensors Actuators B Chem. 249 (2017) 149–155.
[34] S.N. Azizi, S. Ranjbar, J.B. Raoof, E. Hamidi-Asl, Preparation of Ag/NaA zeolite modified carbon paste electrode as a DNA biosensor, Sensors Actuators B Chem. 181 (2013) 319–325.